

RPN77

RADIATION PROJECT PROGRESS REPORT NUMBER 4

SYNCHROTRON RADIATION

by

David C. dePackh and Joachim B. Ehrman

Electron Beams Branch
Plasma Physics Division

and

Terry F. Godlove

Linac Branch
Nuclear Physics Division

5 June 1968

Naval Research Laboratory
Washington, D.C.

RADIATION PROJECT PROGRESS REPORT NUMBER 4

SYNCHROTRON RADIATION

An overview of the synchrotron radiation problem is contained in Radiation Project Progress Report Number 2¹. A discussion of program MAGCOIL for determining the field due to a given conductor geometry (in axial symmetry) is contained in Radiation Project Progress Report Number 3, Parts I and II². Subsequent work on the synchrotron radiation problem has been concerned with

- (1) a general approximate analytical determination of the requirement for a magnetic energy converter, including its relation to the linac beam;
- (2) development of the TRAP program for computer analysis of the problem of single-particle injection into the converter;
- (3) a general examination of the frequency and power requirements for the linac as they depend on beam and cavity parameters;
- (4) an examination of potential rf sources for the linac;
- (5) a preliminary examination of linac instabilities at high beam current;
- (6) studies of electric power transmission across a narrow vacuum gap using a bias magnetic field;

(7) construction of a full-scale magnetic converter to be used with the NRL linac for injection studies (at about 20 MeV electron energy).

These will be taken up in turn.

1. Converter Orbit Considerations

It was shown in Radiation Project Progress Report Number 2 that the containment time of a GeV electron in a megagauss field is of the order of 100 nsec, meaning that unless the system is of great length (and therefore with correspondingly great problems of stored energy, particle focusing, and beam spread), the electron must be constrained to execute approximately the same orbit many times. These requirements are of course closely related to megagauss field technology. If there were ways to generate much larger fields, for correspondingly shorter times, there would be the possibility of reducing particle energy, while increasing the current, and reducing the length of the particle path within the converter. This would in turn open the way toward improving the geometry of the radiation beam. Such techniques are not presently visible, though they bear considering, since most of the cost of this system lies in the generator for the GeV beam. Parapotential flows in highly relativistic beams might, for example, offer a means of generating fields of the order of 10^7 gauss or more in the neighborhood of the anode spot.

These questions are beyond the scope of the present discussion, which, for the reasons given, centers on the idea of a circular converter with conventional weak focusing near the particle orbit, generating in this

neighborhood a field of the order of 10^6 gauss. The problems of the behavior of material conductors producing such a field will form the subject of a future report; here we are concerned only with the question of orbits and of capturing an approximately collimated beam from an approximately monoenergetic source (linac). The beam-produced fields in this situation, even for the highest currents, are much less than those arising from the conductors, so that in a first approximation we consider only single-particle motion.

The field must be shaped to trap particles injected from outside the converter. Therefore outside the region of radial focusing there must be a region of radial defocusing with an unstable equilibrium in between. This state of affairs can be represented by the phase-space diagram of Fig. 1 which shows the separatrix in the R-R plane between stable and unstable orbits. In a time-independent field the incoming orbit must lie on the separatrix for trapping, which then occurs at the saddle point (unstable equilibrium) orbit. In the diagram the separatrix is drawn for a particular field and particle energy; for a given field geometry these determine the positions of the stable and unstable equilibrium orbits. For a field increasing in time, the equilibrium orbit positions move to more widely separated radii and the phase-space area of the separatrix increases. This therefore suggests that particle trapping may occur for initially unstable orbits indicated as type 2 in the figure if the separatrix expands far enough during the trajectory to capture the orbit. Computer calculations show that this indeed the case, and an approximate analysis can indicate roughly what the conditions are for capture. If we neglect all vertical motion and radiation (which is unimportant on the injection time scale) and assume that the motion is mostly azimuthal,

we can write

$$\ddot{R} = c^2/R - (e/\gamma m)H_z$$

on the median plane. Then put $H_z \equiv T(t)h(R/r_0)$, where r_0 is the scale of the field; from adiabaticity arguments we have $\gamma \propto T^{\frac{1}{2}}$. Thus for $\rho \equiv R/r_0$, $d\tau \equiv c dt/r_0$, $\lambda \equiv er_0 T/mc^2 \gamma$, prime $\equiv d/d\tau$, we have

$$d\rho'^2/d\tau = 1/\rho - \lambda h(\rho),$$

so that

$$\frac{1}{2}\rho'^2 = \log \rho - g(\rho) + C, \quad g \equiv \int_0^\rho h(x) dx.$$

The center (stable equilibrium) and saddle point (unstable equilibrium) are given by the solutions of

$$\rho h(\rho) = 1/\lambda.$$

In the interesting region the LHS is a positive function of ρ with a single maximum corresponding to $n=1$ ($n \equiv -r\partial H_z/H_z \partial r$); we denote the saddle point (larger root) by ρ_s . For a given λ the constant C determines the particular orbit (depending on initial conditions). To estimate the range of ρ' values which permit capture (for a given $\rho_1 \equiv$ injection radius), write

$$\frac{1}{2}\Delta\rho'^2 = \int (1/\rho - \lambda h) d\rho,$$

where the integral is along the phase-space orbit. If both ends of

the path are at ρ_s , then

$$\frac{1}{2}\Delta\rho'^2 = -\int \lambda h d\rho = -\left(\int_{\rho_s}^{\rho_{\min}} \lambda h d\rho + \int_{\rho_{\min}}^{\rho_s} \lambda h d\rho \right) \equiv -(\bar{\lambda}_2 - \bar{\lambda}_1) \Delta g,$$

where ρ_{\min} is the least value of ρ encountered on the orbit, $\bar{\lambda}_2$ and $\bar{\lambda}_1$ are appropriate averages of λ over the intervals (ρ_s, ρ_{\min}) along the lower branch and (ρ_{\min}, ρ_s) along the upper branch, and

$$\Delta g \equiv g(\rho_s) - g(\rho_{\min}).$$

Then one can write approximately

$$\frac{1}{2}\Delta\rho'^2 \sim -\lambda \overline{\Delta\tau} \Delta g,$$

where $\overline{\Delta\tau}$ is an appropriate fraction of one turn. This has been estimated by computer calculation to be about 0.3 turns in practical cases, giving

$$\overline{\Delta\tau} \sim 0.3 \times 2\pi \sim 2.$$

Thus the estimated range of ρ'^2 values giving trapped orbits for $\rho_i = \rho_s$ is

$$\left| \frac{1}{2}\Delta\rho'^2 \right| = 2\lambda' \Delta g.$$

In the spirit of this approximate analysis we suppose that when injection occurs, as it generally does, at a radius $\rho_i > \rho_s$, the same value holds for $\rho_i' \Delta\rho_i'$ at injection, that is,

$$\left| \rho_i' \Delta\rho_i' \right| = 2\lambda' \Delta g.$$

From the geometry of the injection system one can show that

$$dy/dx = -\tan\left[\arcsin d\rho/d\tau + \arccos(1-y/\rho_1)\right]$$

in a coordinate system with origin at the point of tangency between the x-axis and the injection circle of radius ρ_1 . From the preceding argument we have as an approximate requirement for capture

$$\rho_s' > \rho_1' > \rho_s' + 2\lambda'\Delta g/\rho_s',$$

where ρ_s' is the value of ρ' on the separatrix at $\rho = \rho_1$. Acceptable phase space boundaries are therefore

$$dy/dx = -\tan\left[\arcsin \rho_s' + \arccos(1-y/\rho_1)\right]$$

and

$$dy/dx = -\tan\left[\arcsin(\rho_s' + 2\lambda'\Delta g/\rho_s') + \arccos(1-y/\rho_1)\right].$$

This phase space is sketched in Fig. 2 for some typical parameters. The height is (in order of magnitude) $2\lambda'\Delta g/\rho_s'$ and the width is ρ_1 . Tilting of the injected radial phase-space figure is required for optimizing the fit, implying the desirability of horizontal convergence of the entering beam. Optimally the required phase space is of the order of

$$2\rho_1\lambda'\Delta g/\rho_s'.$$

Reverting to the unnormalized variables, we have

$$|\rho' \Delta \rho'| = (r_0/c) (\dot{H}/H) \Delta g / h(\rho_i),$$

and therefore the capturable phase space in the horizontal plane is, in cm-radians,

$$S_h = r_i \Delta \rho_i' \sim r_i |\rho_i' \Delta \rho_i'| / \rho_s' = r_i (r_0/c) (\dot{H}/H) \Delta g / h(\rho_i) \rho_s'.$$

The quantities Δg , $h(\rho_i)$, ρ_s' must be found by detailed calculation from the field shape; typically such quantities are of unit magnitude so that in order of magnitude S_h is the injection radius times the relative amount the magnetic field changes in one radian of orbital electron motion. This is the required relation between horizontal injected beam quality and the field rise rate.

The effect of an energy spread in the beam (or, equivalently, the effect of an increase in the magnetic field during the injection period) can be considered by temporarily disregarding the field time-dependence. Thus, at any ρ , ρ_s' can be regarded as a function of $1/\lambda$, which plays the role of an energy, and therefore any value of $1/\lambda$ up to the maximum which is just accepted at $n=1$ is allowed. Accordingly an energy-sensitive angular deflector is required at the injection point so that more energetic particles can enter the converter at larger values of $|\rho'|$. The system needs a deflector with a dispersion ($\equiv d\rho'/d(1/\lambda)$) sufficient to insure that moderate energy spreads (ten to twenty percent) can be accommodated. This does not seem a difficult requirement in principle.

2. The TRAP Code

The purpose of this code is to solve the equations of single-particle motion of an electron in the converter guide field. The latter is found from the geometry of the current-carrying conductors by program MAGCOIL. The results of this problem have been checked against measurement in a full-scale model of the converter and found to agree within experimental error ($\pm 0.5\%$ of maximum field).

The equations considered by TRAP are

$$d\mathbf{p}/dt = -(2/3)\gamma r_e^2 (H^2/mc)\mathbf{p} + e[\mathbf{E} + (1/\gamma mc)\mathbf{p} \times \mathbf{H}],$$

$$d\mathbf{r}/dt = (1/\gamma m)\mathbf{p},$$

$$\gamma = (1 + p^2/m^2c^2)^{\frac{1}{2}};$$

the momentum and position are \mathbf{p} and \mathbf{r} , r_e is the classical electron radius, and \mathbf{E} and \mathbf{H} are the electric and magnetic fields. The radiation term $-(2/3)\gamma r_e^2 (H^2/mc)\mathbf{p}$ is a suitable approximation if strong accelerations are absent, as they are here. The output of MAGCOIL is the "pseudopotential" Ψ , where $T(t)\Psi(\mathbf{r}) = RA_\theta$, R being the polar radius. We assume that there is no electrostatic contribution to \mathbf{E} , so that

$$E_\theta = -(\dot{T}/R)\Psi/c, \quad E_R = E_z = 0; \quad H_R = -\partial A_\theta/\partial z = -(T/R)\partial\Psi/\partial z \equiv -(T/R)\Psi_z(R,z),$$

$$H_z = \partial/R\partial R(RA_\theta) = (T/R)\Psi_R(R,z).$$

It is convenient to use Cartesian coordinates, which give

$$H_x = H_R x/R, H_y = H_R y/R, E_x = -E_\theta y/R, E_y = E_\theta x/R, R = (x^2 + y^2)^{\frac{1}{2}}.$$

In addition the original equation has been normalized for the sake of convenience: $\underline{p} \equiv \beta\gamma/\gamma_0 = p/\gamma_0 mc$, $\tau \equiv 10^9 t$, $G \equiv \gamma/\gamma_0$, $\underline{h} \equiv 10^{-6} H$, $S \equiv 10^{-6} T$. Then putting in the numerical values of the constants, we have

$$\begin{aligned} d\underline{p}/d\tau = & -1.94 \times 10^{-6} S^2 (\Psi_z^2 + \Psi_R^2) R^{-2} G \underline{p} \\ & + (17600/\gamma_0) \left[(\dot{S}_y \Psi/cR^2, -\dot{S}_x \Psi/cR^2, 0) + G^{-1} \underline{p} \times (-S_x \Psi_z/R^2, -S_y \Psi_z/R^2, S \Psi_R/R) \right], \end{aligned}$$

$$d\underline{r}/d\tau = 30G^{-1} \underline{p},$$

$$G = (\gamma_0^{-2} + p^2)^{\frac{1}{2}}.$$

A suitable form for S which contains the essentials of the magnetic field time-program is

$$S = S_0 + 10^{-9} \dot{S}_0 \tau - K\tau^2.$$

Thus the whole set of initial parameters are (1) the six coordinates and momenta, which must be chosen so that $G_0=1$; (2) S_0 , \dot{S}_0 , K ; and (3) the MAGCOIL Ψ -values, determined by tabular interpolation from this program. The object of TRAP is to define the boundary of acceptable phase space in the initial values $(z, P_z, y, P_y, \gamma)_0$ for a given conductor configuration and magnetic field time-dependence.

Numerical results from this code will be the subject of a subsequent report.

3. Linac Parameters

There is an array of reasons (Radiation Project Progress Report Number 2) why a stored-energy linac operating at low frequency is probably the best source of generation of intense synchrotron radiation by magnetic conversion. It is therefore appropriate to see how the linac parameters depend on the beam properties. The quantities used in this estimate are

- (1) the rate of particle energy gain for cavities of length L:

$$dT/dz = T' = eE_0 (\sin \frac{1}{2}\phi_e / \frac{1}{2}\phi_e)$$

where E_0 is the peak electric field (v/cm) in a TM_{010} cavity and ϕ_e is the electrical length;

- (2) the Kilpatrick breakdown criterion (valid at frequencies of interest):

$$E_0 = 1.1 \times 10^6 \lambda^{-0.394}$$

where λ is the free-space wavelength (cm) (this level of field is used as a point of reference, since it is realized that fields well over the Kilpatrick value are attainable);

- (3) the stored-energy criterion:

$$\lambda = 6.8 \times 10^6 [(k/h) i t_0 / T']^{\frac{1}{2}},$$

where k is the ratio of the cavity stored energy to that extracted by the beam (energy quality figure), $h \sim 0.29$ for TM_{010} cavities, i is the beam current (amps), and t_0 is the beam duration (seconds);

(4) the Q-factor:

$$Q = 0.77(\lambda/d)/(2 + 0.77\lambda/L),$$

where d is the skin depth;

(5) the total rf power:

$$P_t = k i T_o / Q,$$

where T_o is the total particle energy gain.

A straightforward manipulation of adjustable constants provides a normalized wavelength μ and total power p which can be specified in terms of the electrical length of a single cavity. The electrical length factors are shown in Fig. 3. To find the actual wavelength and power in a working device these should be multiplied by the appropriate normalizing factors, shown in Fig. 4 for various values of V/V_K , where V is the applied cavity voltage and V_K is the Kilpatrick value. Several points are worth noting: (1) increasing the electrical length of the cavity reduces the required rf power at the expense of increased accelerator length; (2) the beam current does not strongly affect the rf power requirements (although increased current demands a proportionate increase in rf stored energy and therefore in fill time); (3) increases in energy gain per meter demand almost proportionate increases in rf power, but the accelerator becomes shorter, and instability dangers are probably diminished. The original estimates of the order of 1000 megawatts at about $3V_K$ for the cavity voltage and a frequency near 50 MHz are still appropriate.

4. Practical Aspects of Linac Design

The problems of the accelerator design separate naturally into the conventional approach, paralleling Venable³ at Los Alamos, versus the

superconducting linac. Considering first the conventional linac, the main problem is the power source.

We assume the following parameters for the purpose of discussion: accelerating field = 30 MV/m; frequency = 50 MHz; wavelength 3m; total length 40m; total energy 1.2 GeV for 27 half-wavelength cavities; total peak rf power required about 1000 MW. These parameters should not vary by more than 20-30% upon more detailed calculations, unless beam currents greater than 2 to 3 kAmp are desired or cavity length greatly different from 180° is employed.

Three alternatives are considered for the rf power source: (1) Use the largest available tube, within ratings or slightly beyond ratings. This approach would be the most conservative one but also the most costly. It would require little advance testing of the power source. (2) Use a presently available tube well beyond normal ratings, either in a straight-forward circuit or perhaps with an unconventional twist such as pulsing the filament to obtain more power. This method would require a moderate testing program to prove the feasibility and determine the extent of the cost saving. The approach is worth consideration because of the low rf duty cycle. (3) Develop a tube tailored to the need.

Alternative 1: The probable choice of an available power tube used in a conservative manner is the RCA type 4617 (oxide emitter) or the RCA 7835 (thoriated tungsten emitter). Each is capable of peak power in the range 5-10 MW. The 4617 however is only rated at this power level for pulses less than 25 μ sec in duration. For the much longer pulse required in this case, some derating would doubtless be necessary for reasonable tube life. The 7835 has no such problem but on the other hand employs a

24 kW filament, requiring 3 MW continuous power for the filaments. This is an important operating cost factor, but not a prohibitive problem. The new NRL Cyclotron, for example, uses the same continuous power level for magnet excitation. For this alternate the cost of amplifiers would be about \$11M, assuming 108 units at \$100K each.

Alternative 2: Available tubes may be used in an unconventional way. Either of the tubes cited in Alternative 1 may be pushed beyond its published ratings, but in each case some testing would have to be done to find the emission vs tube life. In any event, the 4617 appears to have an upper limit of about 10 MW output. The thoriated tungsten of the 7835, on the other hand, invites the possibility of pulsing the filament with a duration, say, 2-3 times its thermal time constant. The emission capability should be doubled with a 10% filament overvoltage. Thus the 24 kW filament level should be maintained and a 3-5 kW pulse added. In this manner 20 MW output may be possible from this tube. Life would depend on the duty factor of the filament overvoltage and possible thermal and mechanical shock damage. In some such manner as this the amplifier cost might be reduced to about \$6M.

Any study of the use of presently available tubes beyond their normal ratings should also include other tubes from such companies as Machlett or Varian-Eimac.

Alternative 3: One may develop a tube tailored to the need. A design goal of either 20 MW or 40 MW would seem appropriate. This would allow either one or two tubes to power each cavity. Developing a tube for less than 20 MW would not be worth the effort when compared with Alternative 2. The annular beam tube mentioned above is the most likely candidate. Its potential advantages are a large emitting surface, higher

voltage (lower gradients), extreme pentode-like characteristic, high efficiency and relatively few parts⁴. By contrast the RCA type of construction can be described as a large number of small beam-forming tetrodes within one envelope. Accordingly, the cost is relatively high. Furthermore the voltage is limited by the relatively high gradients, especially near the screen grid. The RCA tubes presently cost \$20K - \$25K. To scale such tubes to higher power does not appear to be worth the high cost involved, although of course the tube engineers should be given their day in court.

In summary, the RCA multiple-element approach costs about \$2500/MW; the annular beam tube should cost no more than \$1000/MW and perhaps as little as \$300/MW.

It must be recognized, however, that the primary goal in seeking a higher power tube is not wholly to reduce the tube cost but to reduce the number of amplifiers needed. The tube cost will probably be no more than 25% of the total amplifier cost in any case.

Another variation to the tube ratings problem would be to build the power supplies, modulators, rf drive, etc, for a 20 MW (or 40 MW) tube on the assumption that within a few years it can be made to work at this level. The accelerator would be designed in such a manner that an acceptable beam intensity would be obtained even if the tube produced only 50% of its design goal. The higher power, once obtained, would produce a correspondingly greater beam intensity. The cost of adding the necessary flexibility in the beginning would be minimal, perhaps a few percent of the total cost.

TOTAL COST-CONVENTIONAL LINAC

Preliminary estimates are most easily obtainable from figures supplied by Venable. These indicate the basic cost exclusive of amplifiers to be about \$6M. The cost of the amplifiers will depend on which alternative is followed. For the most conservative case (5 amplifiers per cavity, 7.5 MW each) the added cost would be \$11M. For the projected 40 MW tube development, the added cost would be about \$3M. Thus the grand total lies between \$9M and \$18M, depending on the rf source.

SUPERCONDUCTING LINAC

The advantage, or quality, of a low-temperature linac may be judged by the Q-enhancement, that is, the ratio by which the normal electrical losses are reduced by operation at low temperature. The state of the art at present is approximately as follows:

Present Situation: A number of Q-measurements have been made over the past several years with small, unloaded, single cavities, using both lead and niobium surfaces. Many of these measurements have given rough agreement with theory, indicating Q-enhancements up to 10^5 . However, the Stanford five-foot model accelerator using lead has not worked as well as expected. The first major test yielded 6 MeV and on each subsequent trial the performance deteriorated. Niobium is now considered by the experts to be a more suitable material than lead. In addition to the choice of material, there are many other potential problems such as thermal stability, electrical stability, field emission, surface requirements, trapped magnetic flux, thermal and electrical coupling, residual losses and so on. Most of these problems have been dealt with theoretically and are believed

to be soluble, but progress in the practical realization of a superconducting linac has been slow. It is simply not yet clear what the final Q-enhancement will be for a practical machine. Values as low as 10^4 or 10^3 may have to be accepted.

Variation with Frequency: Another question arises when applying these considerations to the present case. What is the variation of the Q-enhancement with frequency? It appears that no experiments have been done even with lead at frequencies lower than 1000 MHz, and certainly nothing has been done with niobium. This question would need to be answered before proceeding very far. Extrapolation to 50 MHz without proof would be very risky.

Cost Saving? Over-riding all of the above considerations is a more basic one. Suppose that a Q-enhancement of 10^5 is attainable. What would be the cost saving assuming that all of the "engineering" problems could be solved? The rf source would need to supply some 5-10 kW instead of 1000 MW. Using the Stanford estimate of \$1200/watt for the cost of refrigeration at 2°K, one obtains \$6M - \$12M for the total cost of refrigeration. Any Q-enhancement less than 10^5 would increase the cost correspondingly. The cost saving is thus highly questionable. The motivation in the case of the Stanford accelerator is not the cost saving but the possibility of a continuous beam. No such motivation exists in the present application.

5. Preliminary Examination of Linac Instabilities

We have computed the propagation of the TM_{10} mode, defined in cavity 0 by the vector potential with Fourier transform

$$\vec{A}_0(\vec{r}, \omega) = A_0(\omega) \vec{\Psi}_0(\vec{r})$$

where $A_0(\omega)$ is an amplitude function, and

$$\begin{aligned} \left(\vec{\Psi}_0\right)_\rho &= \frac{\pi a}{3.83\ell} J_1' \left(\frac{3.83R}{a} \right) \cos\phi \cos\left(\frac{\pi z}{\ell}\right) \\ \left(\vec{\Psi}_0\right)_\phi &= -\frac{\pi a^2}{(3.83)^2 \ell} \frac{1}{R} J_1 \left(\frac{3.83R}{a} \right) \sin\phi \cos\left(\frac{\pi z}{\ell}\right) \\ \left(\vec{\Psi}_0\right)_z &= J_1 \left(\frac{3.83R}{a} \right) \cos\phi \sin\left(\frac{\pi z}{\ell}\right), \end{aligned} \quad (1)$$

a being the radius of the cavity and ℓ its length, down a chain of identical cavities, and 3.83 the lowest positive zero for J_1 . It is assumed that the walls of a cavity are perfect conductors (this restriction must be relaxed in subsequent work), and that the iris between two adjacent cavities is too small to allow much electromagnetic coupling between cavities (another restriction which will subsequently be relaxed). The current density in the 0th cavity is assumed to be in the z-direction and to be given by

$$J_{z0}(\vec{r}, t) = J \delta(y) \delta\left(x-x_0 \cos\left(\omega\left(t - \frac{z}{c}\right) + \epsilon\right)\right) \quad (2)$$

where ω is a forcing frequency, and x_0 is the force amplitude in cavity 0. The z-velocity of the electrons is taken as c , although it could be taken as having a smaller value. ϵ is a phase constant inserted for convenience. J is a constant having the dimensions of a current.

The displacement of the beam in any subsequent cavity as a result of the forced oscillation in cavity 0 is computed. This can be done as a special case of the general formalism given by Helm⁵, but it was thought worthwhile to do it explicitly, since it is not done by Helm in an explicit way so that the physical significance of the results are clearly exhibited. The paper by Panofsky and Bander⁶, which does treat the beam blowup problem in an explicit way in terms of a simple model, is likewise inappropriate for several reasons. Here we treat the propagation of a specified disturbance in cavity 0 as a function of position down the chain of cavities, not as a function of position and time. (Of course, there is always a sinusoidal time factor with forcing frequency ω .) As in Panofsky and Bander, a single cavity here really represents an entire section of 86 cavities if it is applied to a complicated structure like the SLAC, through naturally SLAC is not the final application we have in mind. Because of the negligible intercavity coupling the beam blowup being considered here is the cumulative or multisection kind where the information is conveyed solely by the electron beam, not the regenerative kind with negative group velocity. We can treat the latter only after we have dropped our restriction of negligibly small irises between cavities.

Let us define

$$\begin{aligned}
 u_0 &\equiv \pi \frac{l}{2} \frac{a^2}{(3.83)^2} \left(1 + \frac{\pi^2 a^2}{(3.83)^2 l^2} \right) \int_0^{3.83} dy \cdot y J_1^2(y) \\
 &= .1274 a^2 l \left(1 + \frac{\pi^2 a^2}{(3.83)^2 l^2} \right)
 \end{aligned} \tag{3}$$

(where the definite integral has the value 1.19). Then the portion of the vector potential in the 0th cavity in the TM_{10} mode is given by

$$\begin{aligned}
 \vec{A}_0(\vec{r}, t) &= \frac{\vec{\Psi}_0(\vec{r})}{\omega_0^2 - \omega^2} \frac{8cl}{u_0} J_0 \left(\frac{3.83x_0}{2a} \right) J_1 \left(\frac{3.83x_0}{2a} \right) \\
 &\times \sin(\omega t + \epsilon) \left\{ \frac{\sin\left(\left(1 - \frac{\omega l}{2}\right) \frac{\pi}{2}\right)}{1 - \frac{\omega l}{\pi c}} - \frac{\sin\left(\left(1 + \frac{\omega l}{\pi c}\right) \frac{\pi}{2}\right)}{1 + \frac{\omega l}{\pi c}} \right\}
 \end{aligned} \tag{4}$$

(where $\vec{A}_0(\vec{r}, t) = \int_{-\infty}^{\infty} d\omega' e^{i\omega' t} A_0(\omega') \vec{\Psi}_0(\vec{r})$).

Let the phase σ of an electron be defined by

$$\sigma = \omega \left(t - \frac{z}{c} \right) + \epsilon,$$

then this electron suffers a change in canonical momentum in the x direction (where e is the charge of an electron)

$$\Delta p_x = \frac{eJl^2}{au_0} \frac{8 \times 3.83}{\pi} \frac{\cos \sigma}{\omega_0^2 - \omega^2} J_1' \left(\frac{3.83x_0 \cos \sigma}{a} \right) \\ \times J_0 \left(\frac{3.83x_0}{2a} \right) J_1 \left(\frac{3.83x_0}{2a} \right) \\ \times \left[\frac{\sin \left(\left(1 - \frac{\omega l}{\pi c} \right) \frac{\pi}{2} \right)}{1 - \frac{\omega l}{\pi c}} - \frac{\sin \left(\left(1 + \frac{\omega l}{\pi c} \right) \frac{\pi}{2} \right)}{1 + \frac{\omega l}{\pi c}} \right]^2 \quad (5a)$$

in passing thru cavity 0, or

$$\Delta p_x = 76.59 \frac{eJl}{a^3 \left(1 + \frac{\pi^2 a^2}{(3.83)^2 l^2} \right)} \frac{\cos \sigma}{\omega_0^2 - \omega^2} J_1' \left(\frac{3.83x_0 \cos \sigma}{a} \right) \\ \times J_0 \left(\frac{3.83x_0}{2a} \right) J_1 \left(\frac{3.83x_0}{2a} \right) \\ \times \left[\frac{\sin \left(\left(1 - \frac{\omega l}{\pi c} \right) \frac{\pi}{2} \right)}{1 - \frac{\omega l}{\pi c}} - \frac{\sin \left(\left(1 + \frac{\omega l}{\pi c} \right) \frac{\pi}{2} \right)}{1 + \frac{\omega l}{\pi c}} \right]. \quad (5b)$$

Let us for now assume (Helm, loc. cit, pg. 5) that the change in canonical x-momentum and the change in kinetic x-momentum are internally equal. (In any particular application, the order of magnitude of the vector potential term contribution which gives the difference between the two must be examined, and if it is not negligible, the canonical and kinetic Δp_x should not be equated.)

Note from Eqs. 2 and 5 that both x and Δp_x contain the factor $\cos \sigma$, and are therefore in phase, or 180° out of phase.

(For $\frac{x_0}{a} \ll 1$, $J_1' \left(\frac{3.83x_0 \cos\sigma}{a} \right) \cong \frac{1}{2}$.) For $\frac{x_0}{a}$ small, since $eJ > 0$,

we have Δp_x and x in phase (instability) if $\omega^2 < \omega_0^2$ (where

$\omega_0^2 \equiv c^2 \left(\frac{\pi^2}{l^2} + \frac{(3.83)^2}{a^2} \right)$ is the natural frequency of the TM_{10} mode

in one cavity) and 180° out of phase (damping) if $\omega^2 > \omega_0^2$. Such an in-phase instability can be cured by simple focusing, provided that ω (the forcing frequency) is kept away from some immediate neighborhood of ω_0 . To consider ω near ω_0 , we must replace the finite Q of a cavity by a finite Q (consider resistivity of the walls). This prevents the singularity $\frac{1}{\omega_0^2 - \omega^2}$ from occurring, but introduces a quadrature component in Δp_x which may not be so simply curable. This will be examined later.

If we assume cavity number to be a continuous variable, then (writing p for p_x)

$$\frac{dx}{dn} = \frac{l}{mc} \frac{p}{\gamma} \quad (6a)$$

$$\frac{dp}{dn} = F_x \quad (6b)$$

where $x(n)$, $p(n)$ here do not represent instantaneous displacement or momentum but the amplitudes of these quantities and where the constant F is given by $\left(\frac{x_0}{a} \ll 1 \right)$

$$F = 36.68 \frac{eJ}{a^4 \left(1 + \frac{\pi^2 a^2}{(3.83)^2 l^2} \right)} \times \frac{1}{\omega_0^2 - \omega^2} \times \left[\frac{\sin \left(\left(1 - \frac{\omega l}{\pi c} \right) \frac{\pi}{c} \right)}{1 - \frac{\omega l}{\pi c}} - \frac{\sin \left(\left(1 + \frac{\omega l}{\pi c} \right) \frac{\pi}{2} \right)}{1 + \frac{\omega l}{\pi c}} \right]^2 \quad (7)$$

Let us make two different assumptions about γ as a function of n , namely $\gamma = \text{const.}$ and $\gamma = bn$ where b is a constant. (If $\gamma = bn$, the initial cavity does not have number 0, but some positive number.) $\gamma = \text{const.}$ gives (for $x(0) = x_0$, $p(0) = 0$)

$$x(n) = x_0 \cosh \left(\sqrt{\frac{F\ell}{m\gamma c}} n \right) \quad (8a)$$

$$p(n) = Fx_0 \sqrt{\frac{m\gamma c}{F\ell}} \sinh \left(\sqrt{\frac{F\ell}{m\gamma c}} n \right) \quad (8b)$$

for $F > 0$, the unstable case. $\gamma = bn$ leads to a solution of the form

$$p = \sqrt{n} \left[c_1 I_1 (2\sqrt{Gn}) + c_2 K_1 (2\sqrt{Gn}) \right] \quad (9)$$

where

$$G \equiv F\ell / (mbc).$$

For large n , Eq. 8 implies a growth of the form $\exp(\text{const. } n)$ while Eq. 9 gives a growth $\exp(\text{const. } \sqrt{n})$. Of course, the slower type of growth in the second case is due to the stiffening of the beam as it is accelerated.

Relaxation of the simplifying assumption of lossless and uncoupled cavities will be the next order of business.

6. Power Transmission to the Converter

The inductance and stored energy of the magnetic converter can be accurately calculated with the MAGCOIL code. It is desirable, however, to design the converter proceeding from a basic two-filament coil in a configuration close to the Helmholtz type, which provides a centrally flat field through terms in R^2 . For reasons of creating an escape path for spent electrons it seems wise to have a very slight increase in the field with radius near the center, followed by a maximum and then the usual decrease needed for orbit stability. To reduce the stored energy as much as possible the conductors of the actual coil should probably be placed approximately on the separatrix for which the equi-pseudopotentials around the filament just reach the median plane. Locating the conductors on lower-lying pseudopotentials, though lowering the inductance, severely restricts the space within the coil and allows no easy injection path; locating them on higher ones, while leaving a lot of room for injection, causes a large inductance increase (Fig. 5). Because of this fundamentally simple geometry the inductance can be estimated to reasonable accuracy without the need for the program. For the full-scale model coil the estimated inductance is about 60 nh, and in order to produce a 10^6 -gauss field at the $n=0.7$ point the required stored energy for 1-GeV electrons is about 6 MJ. This quantity is strongly dependent on particle energy, as is indicated in Fig. 6. This represents a practical consideration which tends to push the linac beam toward lower energies and higher currents.

In any of these systems it is required that the converter field should increase rapidly in time. With the above figures for stored energy

and inductance one finds a current of 10 MA coupled with a rise time of the order of 1 μ sec, so that the required voltage is $\sim 60 \times 10^{-9} \times 10^7 \times 10^6$, or, for order-of-magnitude purposes, 1 MV. One of the principal problems here is to minimize the inductance of the leads to the coil. This indicates close spacing, and there is therefore a problem of breakdown in this region.

An attractive way of overcoming this is through the use of magnetic insulation. In the particular case of an inductive load such as is presented in this situation there are problems connected with the fact that voltage must be applied some time before there is an appreciable flow of current, so that the system is unable to develop its own magnetic insulation as in the case of a resistive or field-emission load. Therefore one must apply in effect a slow bias field prior to application of high voltage. This bias field may result either from a large low-frequency current through the conductor, electrically isolated from the high-voltage supply by a large series inductance, or by a field produced by external conductors. Each of these methods has characteristic advantages and disadvantages. Thus if the bias field is produced by currents within the internal conductor, the magnetic and electric fields tend to become large together (in regions of large curvature), there is no problem in principle in transitions between coaxial and other geometries, and internal magnetic energy is stored only where it is needed. On the other hand, it is necessary to provide isolation between the high and low-voltage systems, which necessitates an external inductance in which much energy must be stored; moreover, there is a difficulty with inductive loads which are not in a vacuum environment arising from the presence of the insulator which separates the vacuum region from the load. Since such an insulator blocks the downstream flow of electrons, it will tend to become charged and thus to deflect the stream into the anode as the system attempts to set up an equilibrium flow⁷. For many geometries the extra

stored energy which must fill regions of low or zero electric field when the insulating field is provided by external conductors is not too high a price for freedom to use downstream insulators and the convenience afforded by complete electrical separation between bias and high-voltage circuits. In a given situation the choice of one or the other method depends on individual circumstances. In any such systems the vacuum must be sufficient to insure that formative spark time \gg pulse length⁸. From the electron drift time $T_{\mu s} = 35H^2 \text{ kg}^2 / P_{\text{Torr}} V_{\text{Volts}}$ given in Ref. 8, we have for $H = 10\text{kG}$, $V = 10^6\text{Volts}$, $P = 10^{-5}\text{Torr}$, $d = 0.5 \text{ cm}$, the formative time $\sim 800\mu s$; this requirement is thus amply satisfied by good vacua.

It is appropriate to examine the question of magnetic insulation in a coaxial geometry with an external coil, since this was not covered in the discussion of parapotential flow⁷. This condition is characteristic of magnetrons, where we suppose \underline{v} , \underline{E} , and \underline{H} to be mutually perpendicular. The equations are

$$dH/dR = 4\pi J,$$

$$\beta = (1-\gamma^2)^{\frac{1}{2}},$$

$$R^{-1}d/dR(Rd\gamma/dR) = 4\pi J/1700\beta,$$

$$\beta^{-1}d\gamma/dR + \beta\gamma/R = H/1700,$$

where $H \equiv H_z$, J is the current density, and the last equation takes account of the centrifugal force. These can be combined to give

$$Rdg/dR = g^2/(\gamma-1/\gamma) + \gamma(\gamma^2-1),$$

$$Rd\gamma/dR = g;$$

thus

$$dg/d\gamma = \gamma[g(\gamma^2-1)^{-1} + g^{-1} + g^{-1}(\gamma^2-1)],$$

giving

$$g = [(\gamma^2-1)^2 + C(\gamma^2-1)]^{\frac{1}{2}},$$

where C is a constant. To determine C we have

$$\begin{aligned} \beta^{-2}(d\gamma/dR)^2 &= R^{-2}\beta^{-2}(\beta^4\gamma^4 + C\beta^2\gamma^2) = R^{-2}(\beta^2\gamma^4 + C\gamma^2) \\ &= (H/1700 - \beta\gamma/R)^2. \end{aligned}$$

For $\beta \rightarrow 0$, $H \rightarrow H_0$ (field at the cathode), so that

$$C = (r_0 H_0 / 1700)^2.$$

One finds then

$$d\gamma/d \log R = [(\gamma^2-1)^2 - C(\gamma^2-1)]^{\frac{1}{2}},$$

so that

$$\Delta \log R = \log R/r_0 = \frac{1}{2} \int_0^{\hat{P}} dP/[P(P+1)(P+C)]^{\frac{1}{2}},$$

where $P \equiv \gamma^2-1$; \hat{P} is the maximum value of P.

According to Abramowitz and Stegun⁹

$$\log R/r_0 = C^{-\frac{1}{2}} F(\arcsin \sqrt{P/(P+1)}, \sqrt{(C-1)/C}),$$

or

$$\hat{\gamma} = 1/\operatorname{cn}(C^{\frac{1}{2}} \log \hat{R}/r_0),$$

where the circumflex refers to the outside electron. We must have $C \geq 1$ for a possible flow. Generally F is not too different from an arc cosine of $1/\gamma$ except for very large C , and the interesting behavior is reasonably well represented by the formula

$$C^{\frac{1}{2}} \log \hat{R}/r_0 \sim \arccos 1/\hat{\gamma}.$$

One should of course note that C refers to the field inside the flow, and that on the outside (produced by the external coil) will be higher, the value being

$$\hat{H} = 1700(\hat{\beta} \hat{\gamma}/\hat{R} + \beta^{-1}(d\hat{\gamma}/dR)).$$

Thus

$$\hat{H}\hat{R}/1700 = \hat{\beta} \hat{\gamma} + \hat{\beta}^{-1}(\hat{\beta}^4 \hat{\gamma}^4 + C\hat{\beta}^2 \hat{\gamma}^2)^{\frac{1}{2}}.$$

For large γ we have in order of magnitude $C^{\frac{1}{2}} \sim 1/\log \hat{R}/r_0$.

In order to check out these ideas we have built a test section which can be connected to the 40-ohm Blumlein previously used for diode testing.¹⁰

This will be fitted with an isolating inductance for direct connection to the low-voltage bank as well as having provision for an external coil. (Fig. 7). Interelectrode spacings of 1.0 and 0.5 cm will be tried in this arrangement. They will be subjected to about 1 MV.

7. Magnetic Converter for the NRL Linac

It was decided that, as a supplement to the TRAP code, an attempt would be made to examine the radiation produced by capturing the beam from an existing linac at moderate energy (NRL machine) using a full-scale model of the final converter (Fig. 8). The conductor shape used in the coil was derived from a two-filament configuration with a separation-to-radius ratio of 0.45. Starting with the analytical formula for the pseudopotential, involving complete elliptic integrals, the separatrix surface was sketched and then fitted with a simple curve made up of straight lines and circular arcs (Fig. 9). The final check was made by using the manufactured cross sectional shape as input to MAGCOIL and comparing this with measurement. (Fig. 10).

The particular parameters of the experiment were determined by convenience in the stored-energy source for driving the coil. This is a 2-kJ fast (20 ns) condenser with a capacity of 2 μf (manufactured by Sangamo). The estimated total circuit inductance is 100 ns, providing a peak field at the orbit position of ~ 20 kG and a ringing period of about 3 μsec . With the design orbit at 3.4 cm radius this specifies an electron energy of 20 MeV. The indicated parameters also provide a critical energy of 1.7 eV and characteristic synchrotron radiation time of 0.03 sec, leading to a radiation loss rate of 10^{-10} watts per electron. If at first approximation it is assumed that the capture interval of the

magnetic field is $1/2\pi$ times the ringing period, or $\sim 4 \times 10^{-7}$ sec, and that the accelerator delivers beam to the coil at 10 mA, one gets a rate of power generation by synchrotron radiation (at all angles) of 2.4 watts. The spectrum roughly resembles that of a black body at a temperature of about 0.1 of the critical energy, or $0.17 \text{ eV} \sim 2000^\circ\text{K}$. These figures represent a high input for a photomultiplier tube and may therefore permit substantial collimation of the linac beam so that accurate determination of injection conditions will be possible for quantitative comparison with TRAP. The experimental layout is shown in Fig. 11.

The first phase of this study will be completed when (1) satisfactory results from TRAP, hopefully confirmed by experiment, are in; (2) when satisfactory operation of the low-impedance power transfer system for the converter has been achieved; and (3) when a reasonable estimate of beam stability can be made.

REFERENCES

1. D. C. dePackh, "Preliminary Report on the Investigation of Synchrotron Radiation as a Potential Source of Intense Electromagnetic Energy," Radiation Project Progress Report Number 2, December 21, 1967, 001290/RD.
2. R. T. Close, "Computer-Assisted Magnetic Field Design - Part I," 7 March 1968, "Computer-Assisted Magnetic Field Design, 'Users' Notes for Program MAGCOIL' - Part II", 10 April 1968, Radiation Project Progress Report Number 3.
3. D. Venable, et al., "Phermex: A Pulsed High-Energy Radiographic Machine Emitting X-Rays," Los Alamos Report LA-3241, May 1967.
4. D. Priest, "Prospects for Very High Power, High Efficiency RF Generator," paper presented at Cambridge University, September 1966.
5. R.H. Helm, Stanford Linear Accelerator Publication 218, see also 1966 Linac Conference LA-3609.
6. W.K.H. Panofsky and M. Bander, Stanford Linear Accelerator Publication 342.
7. D.C. dePackh, "Parapotential Electron Flow and the Vacuum Pinch," Radiation Project Internal Report Number 7, 19 April 1968.
8. A. Sherwood and W. Kunkel, Journal of Applied Physics, 39, p. 2343, April 1968.
9. M. Abramowitz and I. Stegun, Handbook of Mathematical Functions, Dover Publishers, page 597, 1965,
10. J.J. Condon, "Measurement of Bremsstrahlung Radiation Produced with High-Current Diodes and Coaxial Blumlein Generators," Radiation Project Progress Report No. 6, to be published.

FIGURE CAPTIONS

1. Schematic of radial phase space of magnetic energy converter.
2. Limits of horizontal acceptance in magnetic converter for typical parameters (A and B) and approximately matching linac phase space (ellipse).
3. Cavity electrical length factors (K_g and K_e determined from Fig. 4).
4. Power and wavelength factors (V_K is the Kilpatrick breakdown voltage). These numbers multiplied by the appropriate values found from Fig. 3 provide total power and wavelength for a 1-GeV accelerator. (k/h is an energy quality factor).
5. Lines of constant magnetic pseudopotential for Helmholtz geometry.
6. Interrelationship of critical energy, containment time, magnetic field, electron energy, and magnetic stored energy based on present coil design.
7. Layout of magnetic insulator test section.
8. The model converter.
9. Cross section of converter.
10. Comparison of measured and theoretical converter field.
11. Layout of linac beam-capture experiment.

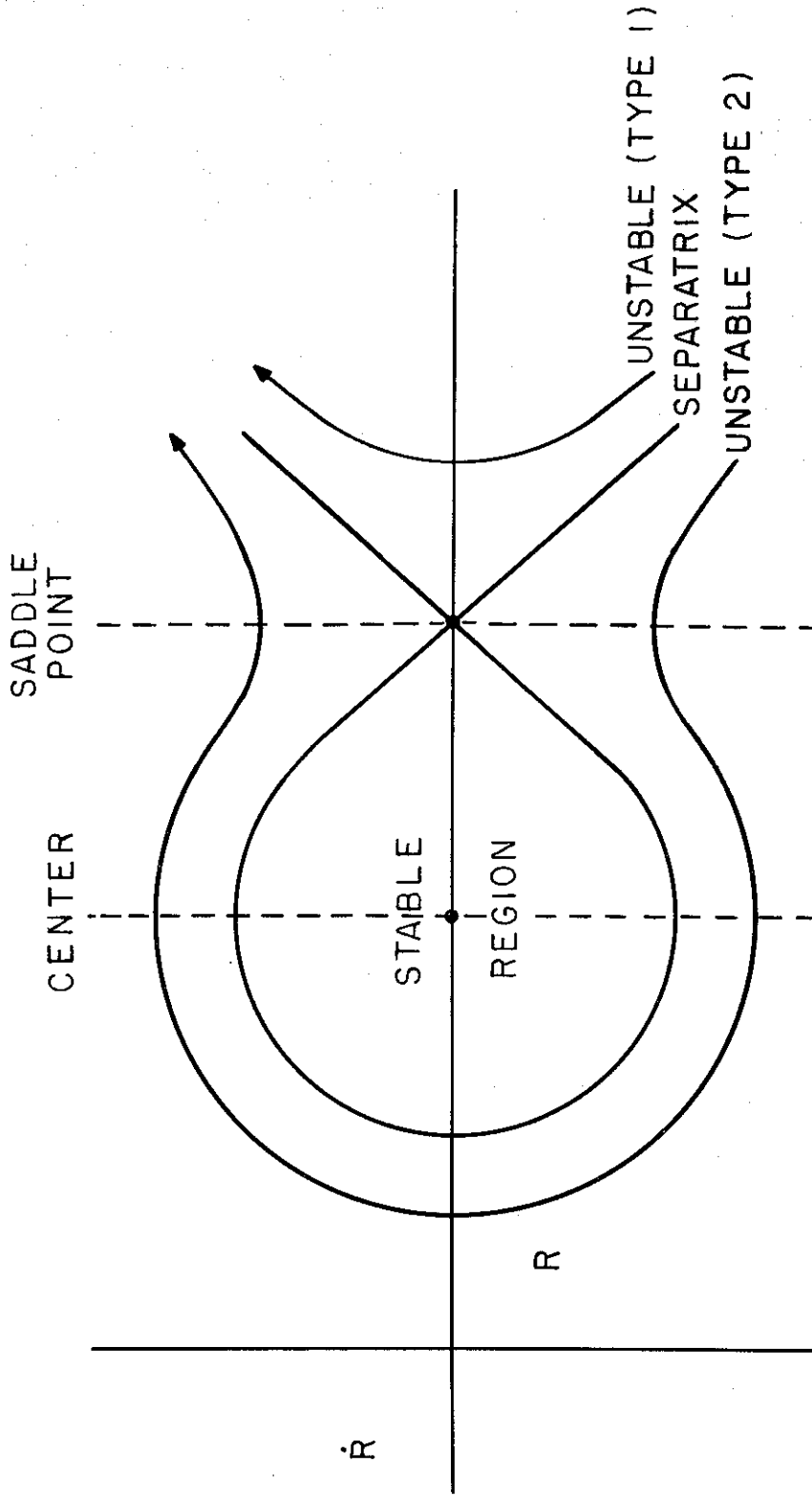


Figure 1 - Schematic of radial phase space of magnetic energy converter.

Figure 2 - Limits of horizontal acceptance in magnetic converter for typical parameters (A and B) and approximately matching linac phase space (ellipse).

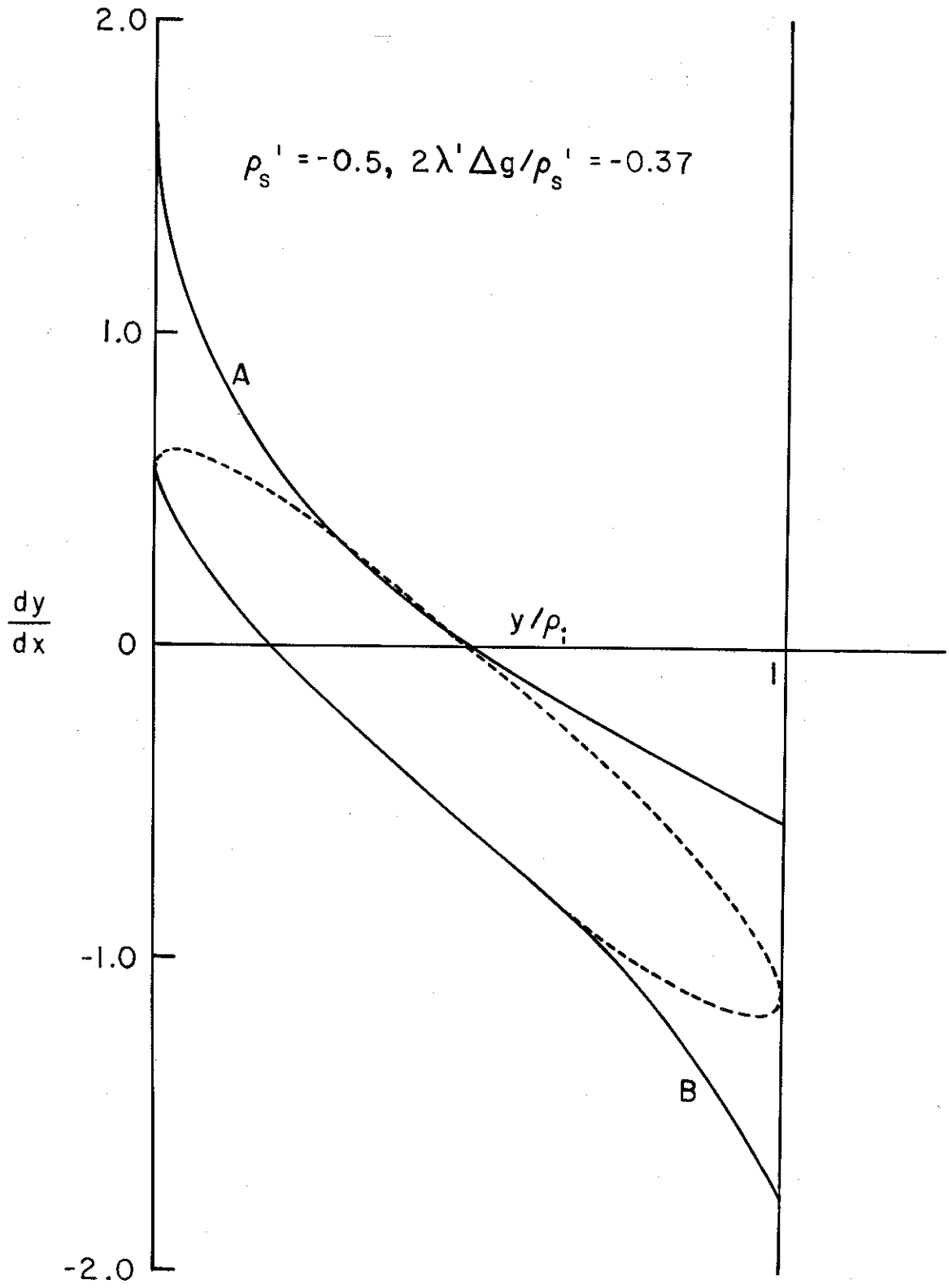


Figure 3 - Cavity electrical length factors (K_3 and K_5 determined from Fig. 4)

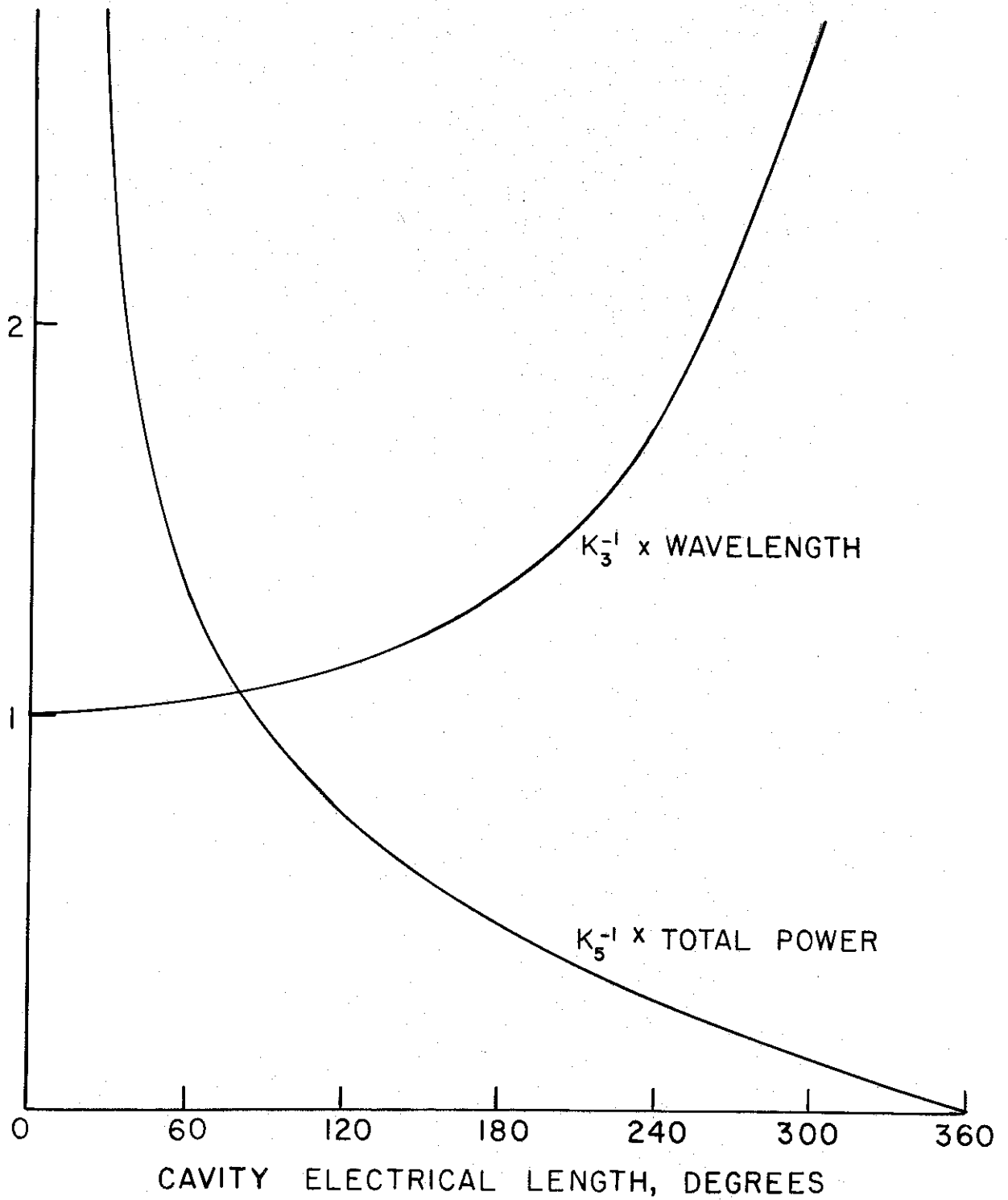
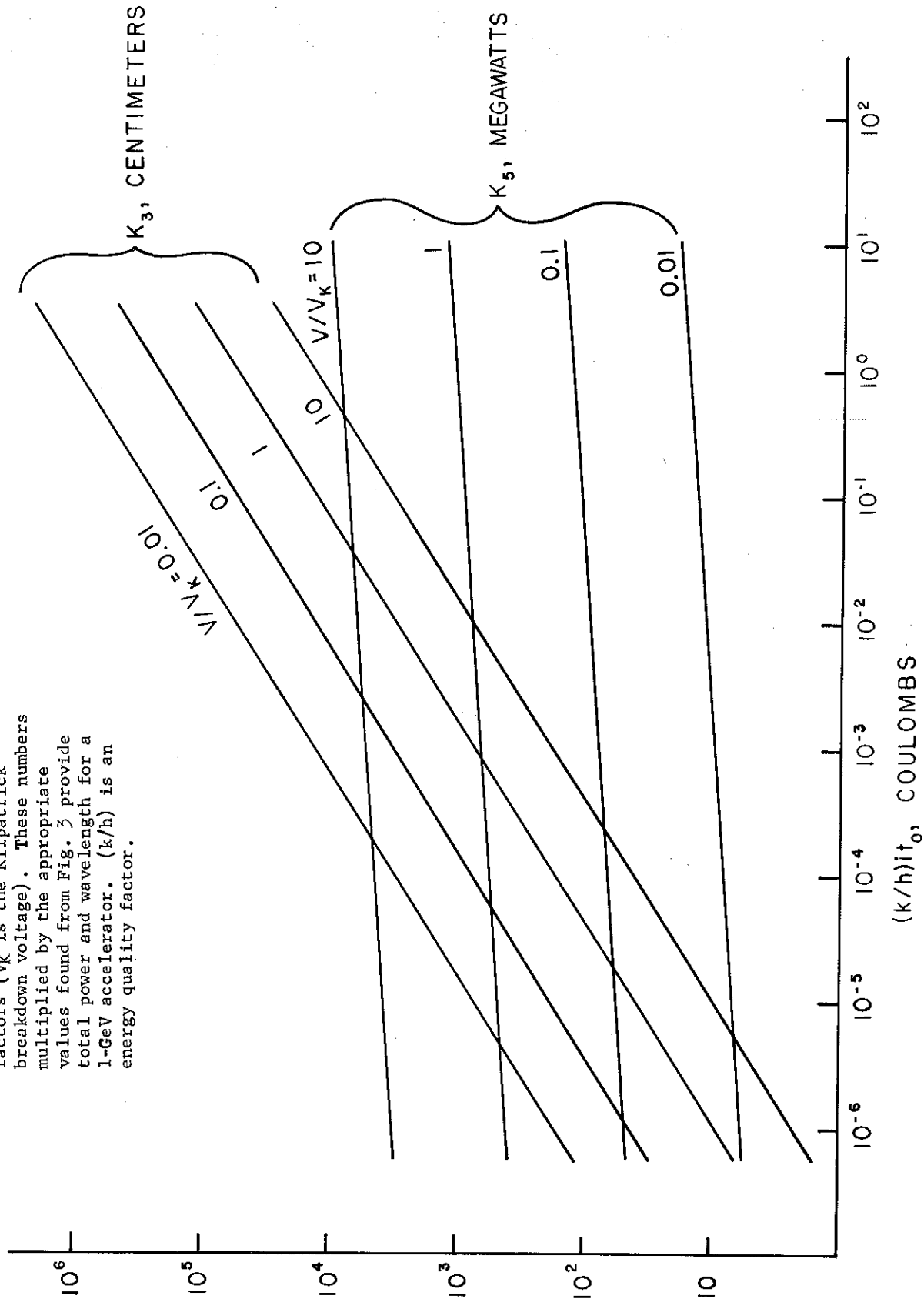


Figure 4 - Power and wavelength factors (V_k is the Kilpatrick breakdown voltage). These numbers multiplied by the appropriate values found from Fig. 3 provide total power and wavelength for a 1-GeV accelerator. (k/h) is an energy quality factor.



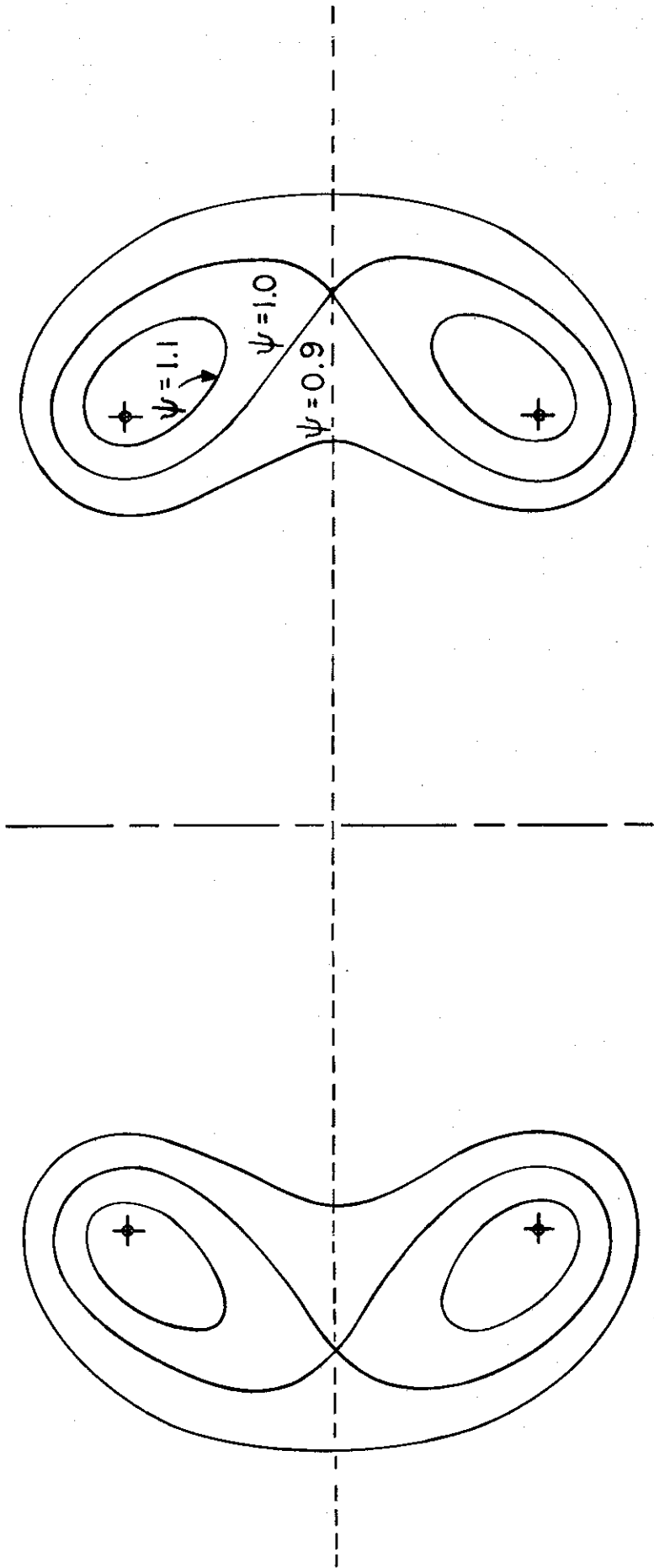


Figure 5 - Lines of constant magnetic pseudopotential for Helmholtz geometry.

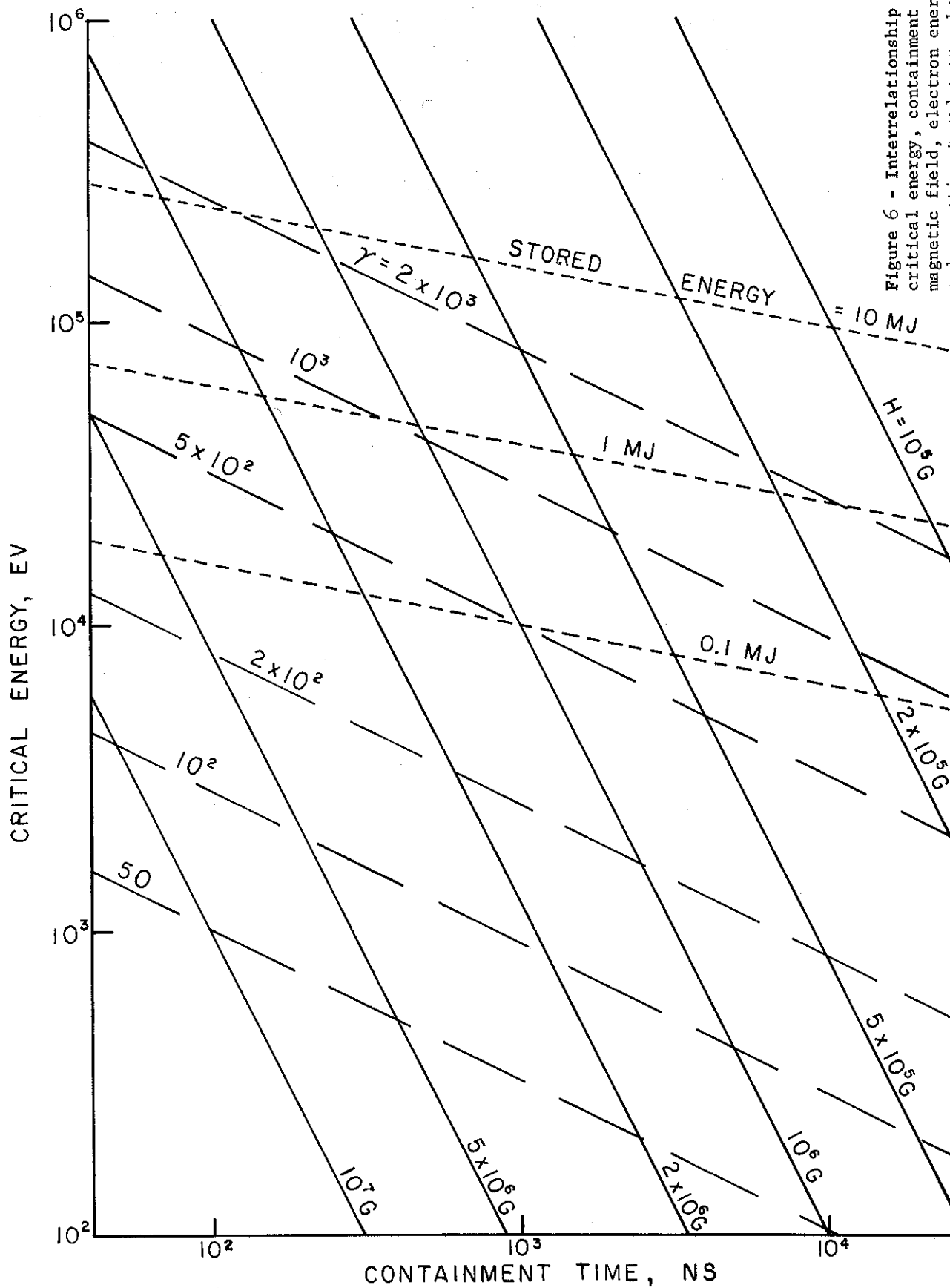
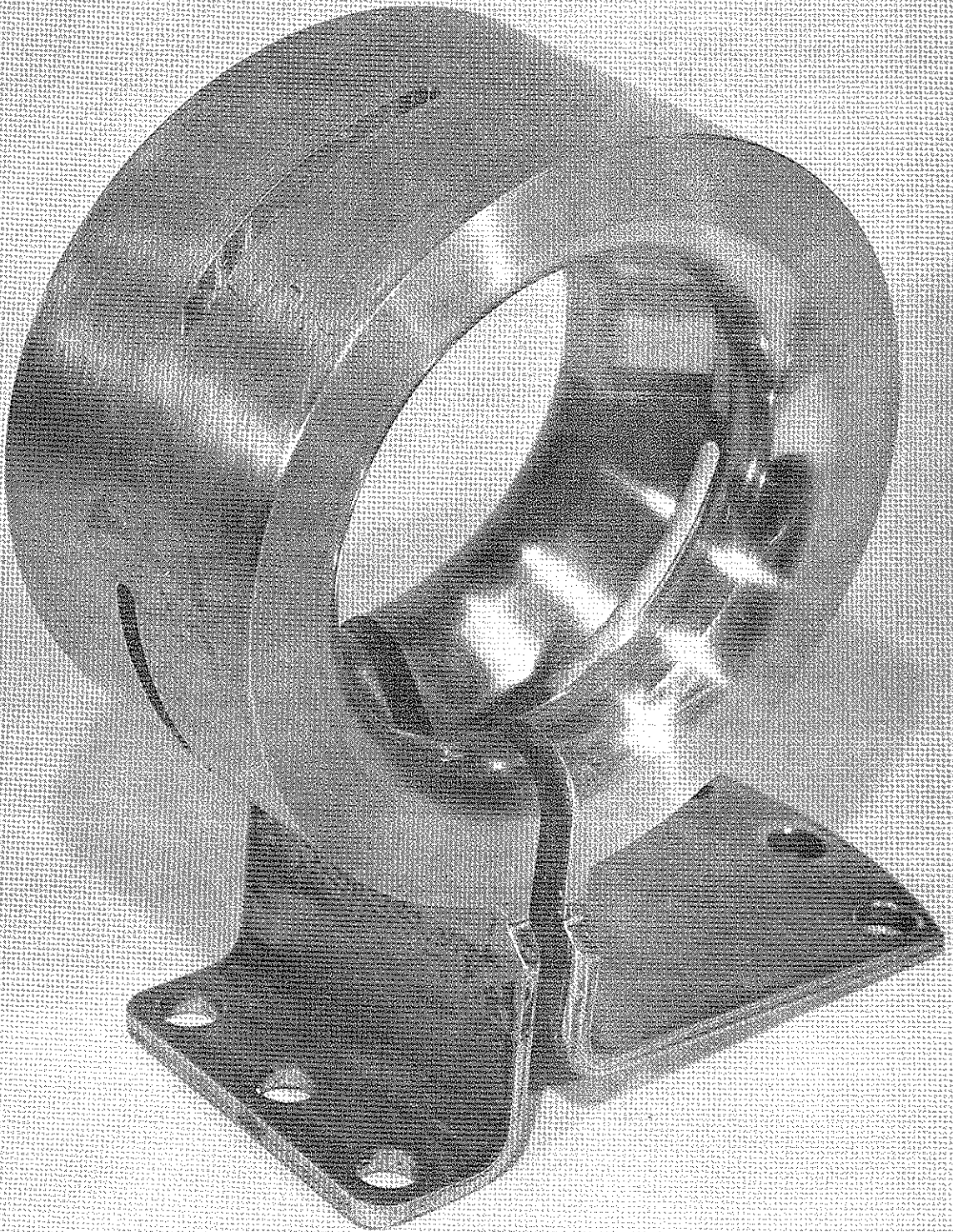
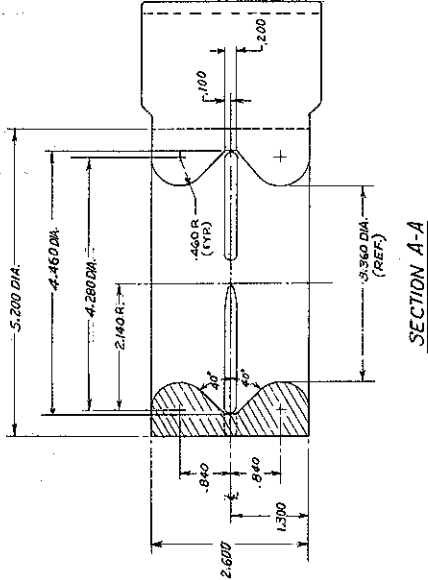


Figure 6 - Interrelationship of critical energy, containment time, magnetic field, electron energy, and magnetic stored energy based on present coil design.

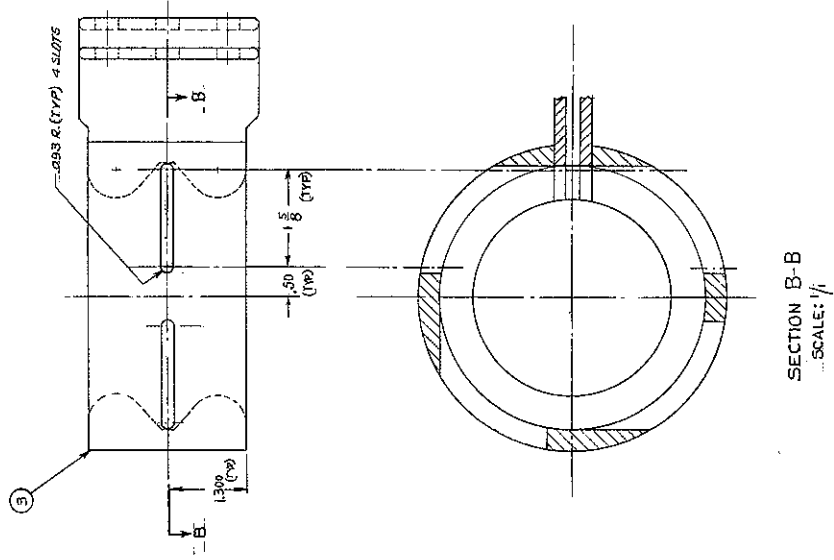


REVISED BY	REVISIONS DESCRIPTION	DATE APPROVED



SECTION A-A

(2) MATL: BRASS
1 REQ'D.



SECTION B-B
SCALE: 1/1

PART NO.	DESCRIPTION	SPECIFICATION	QTY	RECD.
3	5.200 DIA. X 2.600 WIDE	BRASS	1	
2	SUB-ASSEMBLY		1	

PARTS LIST	
E.S.D. ENGINEER	NAVAL RESEARCH LABORATORY
ALDO J. ...	ENGINEERING SERVICES DIVISION
...	WASHINGTON, D.C. 20390
DESIGN	SYNCHROTRON RADIATION
E.S.D. ...	LINAC EXPERIMENT
BRANCH	MAGNETIC FIELD COIL DETAILS
APPROVED BY	DWG. NO. D-004-439
DATE	SCALE LISTED

UNLESS OTHERWISE SPECIFIED DIMENSIONS ARE IN INCHES TOLERANCES ON DIMENSIONS ARE FRACTIONS DECIMALS ANGLES DO NOT SCALE DRAWING

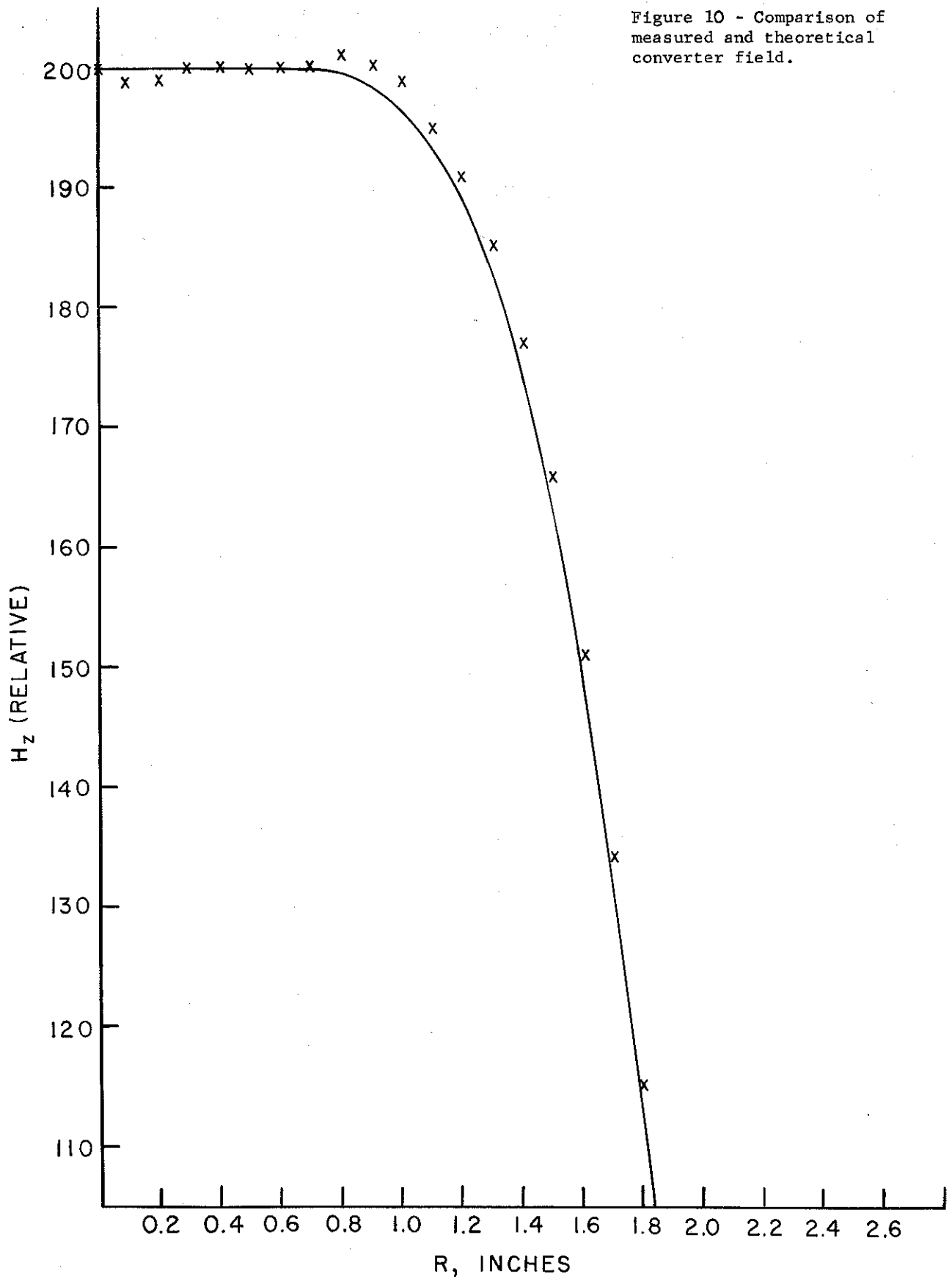
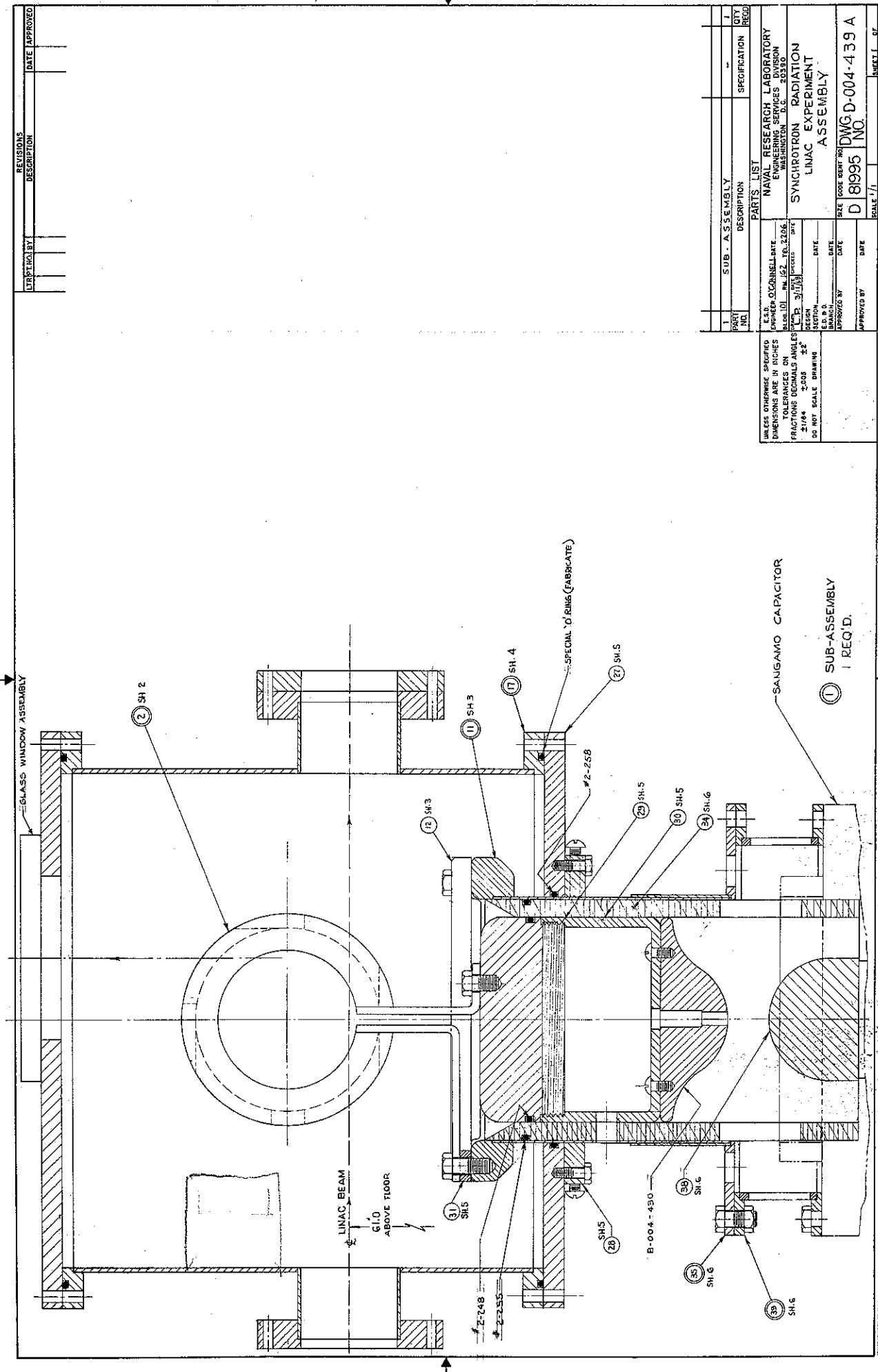


Figure 10 - Comparison of measured and theoretical converter field.



REVISED BY	DATE APPROVED

REVISIONS	DESCRIPTION	DATE APPROVED

NO.	DESCRIPTION	DATE

NO.	DESCRIPTION	DATE

NO.	DESCRIPTION	DATE

NO.	DESCRIPTION	DATE

NO.	DESCRIPTION	DATE

NO.	DESCRIPTION	DATE

NO.	DESCRIPTION	DATE

NO.	DESCRIPTION	DATE

UNLESS OTHERWISE SPECIFIED
DIMENSIONS ARE IN INCHES
TOLERANCES ON
FRACTIONS DECIMALS ANGLES
2/164 2/108 2/2
DO NOT SCALE DRAWING

E.S.O.
ENGINEER
DATE
DESIGN
SECTION
BRANCH
APPROVED BY
DATE

NAVAL RESEARCH LABORATORY
ENGINEERING SERVICES DIVISION
WASHINGTON, D.C. 20390

SYNCHROTRON RADIATION
LINAC EXPERIMENT
ASSEMBLY

SIZE
D 81995
NO. DWG-D-004-439 A

SCALE 1/1

SHEET 1 OF

① SUB-ASSEMBLY
1 REQ'D.